

Overloading behavior of fenoprofen and naproxen as two model compounds on a non-porous silicon pillar array column

Naghdi, Elahe; De Malsche, Wim

Published in:
Journal of Chromatography A

DOI:
[10.1016/j.chroma.2021.462332](https://doi.org/10.1016/j.chroma.2021.462332)

Publication date:
2021

License:
CC BY-NC-ND

Document Version:
Accepted author manuscript

[Link to publication](#)

Citation for published version (APA):
Naghdi, E., & De Malsche, W. (2021). Overloading behavior of fenoprofen and naproxen as two model compounds on a non-porous silicon pillar array column. *Journal of Chromatography A*, 1651, [462332]. <https://doi.org/10.1016/j.chroma.2021.462332>

Copyright

No part of this publication may be reproduced or transmitted in any form, without the prior written permission of the author(s) or other rights holders to whom publication rights have been transferred, unless permitted by a license attached to the publication (a Creative Commons license or other), or unless exceptions to copyright law apply.

Take down policy

If you believe that this document infringes your copyright or other rights, please contact openaccess@vub.be, with details of the nature of the infringement. We will investigate the claim and if justified, we will take the appropriate steps.

Overloading behavior of fenopufen and naproxen as two model compounds on a non-porous silicon pillar array column

Elahe Naghdi^{1,2}, Wim De Malsche^{1*}

1. μ Flow group, Department of Chemical Engineering, Vrije Universiteit Brussel, Pleinlaan 2, 1050 Brussels, Belgium.
2. Faculty of Chemistry, Shahid Beheshti University, G.C., Tehran, I.R. Iran.

(*) corresponding author

Pleinlaan 2, B-1050, Brussels, Belgium

Tel.: +32 (0) 2 629 3781, Fax.; +32-2 629 3248, E-mail: Wim.De.Malsche@vub.be

Abstract

In this study, the adsorption behavior of naproxen and fenopufen as two model compounds on a non-porous pillar array column (NPAC) was investigated under reverse phase liquid chromatography conditions. Band profiles of both analytes were recorded in overloaded concentrations using 30% methanol/water (v/v) as the mobile phase. Breakthrough experiments under the same chromatographic condition were carried out to measure the adsorption isotherms. Single-component adsorption isotherm data were acquired by frontal analysis for each analyte.. The isotherms were found to be concave upward and downward for naproxen and fenopufen, respectively. To find the best agreement between the experimental data points and the adsorption isotherm models, the obtained isotherms were modeled using several isotherm models. The Langmuir-Freundlich and anti-Langmuir models provided the best fitting for fenopufen and naproxen, respectively. The solute and stationary phase properties determine the appropriate model. Adsorbate-adsorbate interaction is important in the case of naproxen, while the adsorbate-adsorbent (stationary phase) plays the main role in retention of fenopufen on the NPAC. The validity of the selected isotherm models were checked comparing calculated and experimental band profiles and plate heights. An excellent agreement was observed for the whole concentration range of both analytes, which confirmed the accuracy of the selected models.

Keywords: Adsorption isotherm; Anti-Langmuir model; Equilibrium-dispersive model; Langmuir-Freundlich model; Non-porous pillar array;

29 **1. Introduction**

30 Preparative chromatography is one of the most powerful separation processes for the purification
31 of valuable and pharmaceuticals products [1-3]. Chromatography is often preferred because the
32 process allows for both high yields and purities.

33 The optimization of a chromatographic separation process at a preparative scale is generally a
34 complex task and requires a careful selection of the operation conditions. Therefore, ideally, one
35 of the first steps in studying this process is the determination of the equilibrium adsorption
36 isotherms of the analytes. This allows gaining insight in the retention mechanism and to predict
37 and evaluate the production rate recoveries and eventually separation costs [4].

38 Purification of large sample amounts by preparative high performance liquid chromatography
39 (HPLC) is possible using two methods: 1) scale-up of the analytical system, 2) working at maximal
40 concentration. Scale-up of the analytical system implies using a larger column and higher flow
41 rate of mobile phase.

42 Column overloading can occur through (a) volume overloading or (b) concentration overloading.
43 In concentration overload, a small volume of the sample is injected, but its concentration exceeds
44 the linear range of the adsorption isotherm. As a result, the band profile broadens and becomes
45 unsymmetrical. Concentration overloading has been reported to purification of various compounds
46 for which there is an interest to purify, as. e.g. phosphorothioated oligonucleotides [5], anthocyanin
47 glucoside cinnamic ester isomers [6] and peptides [7].

48 The adsorption isotherm at equilibrium between the amounts adsorbed in the stationary phase and
49 the concentration in the mobile phase determines the direction of the band asymmetry, either as a
50 fronting or tailing shape. The overload band profiles and related the adsorption isotherms in reverse
51 phase liquid chromatography (RP-LC) conditions using packed [8,9] and monolithic [10,11]
52 columns have been studied to understand of retention and overloading mechanisms.

53 Pillar array columns (PACs) have been introduced as an alternative column format to packed bed
54 and monoliths in analytical liquid chromatography (LC) and have shown to yield high peak
55 capacities and column efficiencies. Recently, porous PACs have been successfully used to
56 separation of chiral and non-chiral compounds [12-14]. From the point of view of minimizing

57 dispersion (and peak capacity) however, non-porous support structures are fundamentally superior,
58 and typically produce a double plate count of what is achieved for the same non-porous column
59 [15], when working at low concentration is possible (e.g. due to detection sensitivity constraints).
60 When the analytes are large (e.g. DNA or RNA strands or large proteins), it is not desirable to have
61 the large analyte molecules entering similarly sized pores, which leads to excessive dispersion.
62 Using non-porous silicon pillars allowed for high resolution separation of DNA strands in ion-pair
63 reversed phase chromatography mode [16].

64 Several applications with non-porous PACs (NPACs) using small molecules have been reported
65 as well [17, 18]. Even for analytical purposes it is instrumental to understand overloading behavior,
66 as detection limits (or statistical considerations) generally requires for at least a few components
67 to work at overloading conditions. In the present study, we investigated the application of NPAC
68 in concentration overloading conditions. Two commonly used non-steroidal anti-inflammatory
69 drugs (naproxen and fenoprofen) were selected as representative analytes. To gain a better
70 understanding in the general retention mechanism of these two compounds in RP-LC using
71 NPACs, the single-component adsorption isotherms of the analytes were measured by frontal
72 analysis. The adsorption isotherms were modeled by anti-Langmuir and Langmuir-Freundlich
73 models for naproxen and fenoprofen, respectively. This information is subsequently used to
74 estimate band profiles at given concentrations.

75 **2. Theory**

76 **2.1. Determination of the single-component adsorption isotherms by frontal analysis method**

77 Frontal analysis (FA) is an accurate method [19] that allows for in-situ measurement (in the intact
78 separation column), and is the method of the choice when very small amounts of stationary phase
79 are available (or when the stationary phase material is embedded and cannot be separately prepared
80 or isolated, as in the case of PACs). In FA, the breakthrough curves are recorded by the successive
81 replacement of the stream of mobile phase through the column with streams of sample solutions
82 of increasing concentrations.

83 Mass conservation of the solute between the times when the new solution enters the column and
84 when the plateau concentration is reached allows for the calculation of the mass of solute retained

85 in the column at equilibrium (m_t^*) with the sample concentration in mobile phase (C). This mass
86 is measured by integrating the breakthrough curve [20]:

$$87 \quad m_t^* = CV_{eq} \quad (1)$$

88 where V_{eq} indicates the elution volume of the equivalent area of the solute.

89 The amount of adsorbed solute on the stationary phase (q^*) at equilibrium with a sample
90 concentration in the mobile phase is given by:

$$91 \quad q^* = (m_t^* - C V_0)/V_a \quad (2)$$

92 V_0 and V_a show the column void volume and the volume of stationary phase, respectively. V_0 was
93 determined from the elution time of uracil as a non-retained compound. The information on the
94 adsorption behavior is captured in the set of pairs q^* and C.

95 **2.2. Modeling of the single-component adsorption isotherms**

96 After the experimental evaluation of the adsorption data, an isotherm model is useful to interpret
97 the adsorption behavior and the overall chromatographic process. Langmuir-Freundlich and the
98 anti-Langmuir models were used to describe the adsorption isotherm of fenoprofen and naproxen,
99 respectively. The Freundlich-Langmuir isotherm equation is given by [21]:

$$100 \quad q^* = q_s K C^{1/n}/(1+ K C^{1/n}) \quad (3)$$

101 where q_s , K and n indicate the column saturation capacity, binding constant and heterogeneity
102 index, respectively.

103 The anti-Langmuir isotherm equation is given by [22]:

$$104 \quad q^* = aC/(1-bC) \quad (4)$$

105 with a and b numerical coefficients.

106 **2.3. Modeling of band profiles in HPLC**

107 The overloaded band profiles of naproxen and fenoprofen were calculated using the equilibrium-
108 dispersive (ED) model of chromatography. In this model, the mass balance equation for a single
109 component is written:

$$110 \quad \frac{\partial C}{\partial t} + u \left(\frac{\partial C}{\partial z} \right) + F \left(\frac{\partial q^*}{\partial t} \right) = D_a \left(\frac{\partial^2 C}{\partial z^2} \right) \quad (5)$$

111 where q^* and C are the stationary and mobile phase concentrations of the adsorbate at equilibrium,
112 respectively, t the time z the distance along the column, D_a the axial dispersion coefficient u the
113 linear mobile phase velocity, F the phase ratio defined by $= V_a/V_0$. q^* which is related to C by the
114 isotherm equation [23].

115 The following initial and boundary conditions are used to solve equation 5.

116 At $t = 0$, the concentration of the solute in the column is equal to zero:

$$117 \quad C(0, z) = 0 \quad (6)$$

118 The boundary condition at the column inlet is defined as:

$$119 \quad C(t, 0) = C_i \quad \text{for} \quad 0 < t < t_p \quad \text{and} \quad C(t, 0) = 0 \quad \text{for} \quad t > t_p \quad (7)$$

120 with t_p the injection time of a rectangular injection plug.

121 The boundary condition at the column outlet is:

$$122 \quad \left(\frac{\partial C}{\partial z} \right) = 0 \quad \text{at} \quad z = L \quad \text{and} \quad t > 0 \quad (8)$$

123 The ED model was solved using the finite difference method [24].

124 **2.5. Calculations of the chromatographic figures of merit**

125 The peak asymmetry factor is a measurement of the peak tailing or fronting. The statistical
126 moments are used for calculation of the asymmetry factor (As):

$$127 \quad As = (\mu_1 - t_R) / \sqrt{\mu_2} \quad (9)$$

128 with t_R the retention time of the peak, μ_1 the first statistical moment and μ_2 the second statistical
129 moment. For tailing peaks, the asymmetry factor is positive ($As > 0$) while negative asymmetry
130 ($As < 0$) indicates fronting peaks.

131 The theoretical plate height (H) was calculated using the following equations:

$$132 \quad N = t_R^2 / \mu_2 \quad (10)$$

$$133 \quad H = L / N \quad (11)$$

134 with N and L theoretical plate numbers and the column length, respectively.

135 **3. Experimental**

136 **3.1. Material**

137 Fenoprofen and uracil were purchased from Sigma-Aldrich (St. Louis, MO, USA). Naproxen
138 reference standard was kindly provided by Temad Company (Tehran, Iran). Anhydrous toluene
139 was purchased from Sigma-Aldrich (Overijse, Belgium). Octadecyldimethyl-N,N
140 dimethylaminosilane (ODS-DMA) was purchased from ChemPur Feinchemikalien und
141 Forschungsbedarf GmbH (Karlsruhe, Germany). Purified water from a Milli-Q reagent water
142 system (Billerica, MA, USA) was used to prepare mobile phase and reagent solutions. LC/MS
143 grade methanol and acetonitrile were also obtained from Biosolve (Valkenswaard, Netherland).

144 **3.2. Apparatus**

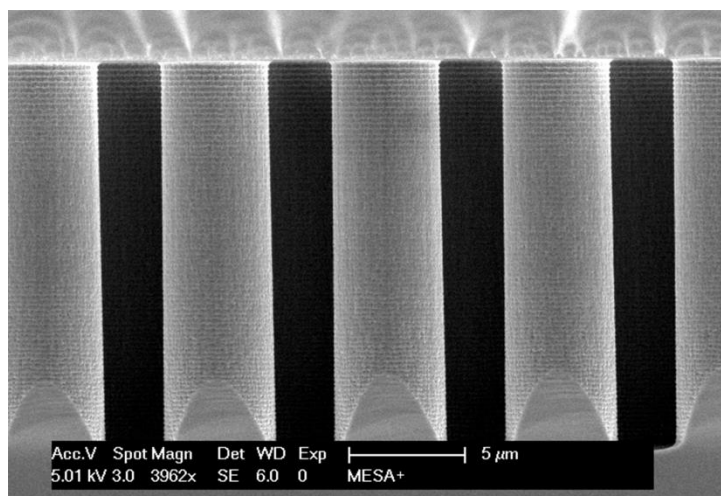
145 A Thermo Fisher Scientific Ultimate 3000 nano-LC system (Germering, Germany) equipped with
146 a membrane degasser, LPG-3600 pump, FLM-3200 column oven, and a VWD-3400 RS UV-
147 detector system was used for chromatography evaluation. The UV system was set at 215 nm for
148 detection of fenoprofen and 230 nm for detection of naproxen. A 4 nl sample injector obtained
149 from Valco (Schenkon, Switzerland) was employed for injection of samples. Data collection and
150 processing were done by the Chromeleon software.

151 **3.3. NPAC fabrication procedure**

152 A 20 cm long and 315 μm wide pillar-array channel (5 μm diameter pillars, inter-pillar distance
153 2.5 μm) was patterned using normal UV photolithography (photoresist, Olin 907-12), followed by
154 a dry etching step (Adixen AMS100DE, Alcatel Vacuum Technology, Culemborg, The

155 Netherlands) to etch the 200 nm thick SiO₂ hard mask underneath. Next, the capillary channels
 156 were defined by subsequent mid-UV lithography, etching of the SiO₂ layer by a Bosch-type deep-
 157 reactive-ion etching step (Adixen AMS100SE) reaching a depth of 80 μm. After this, the resist
 158 was removed by oxygen plasma and nitric acid, and the pillars defined in the SiO₂ mask (and also
 159 the already defined and partly etched capillary groove) were subsequently Bosch etched to reach
 160 a depth of 18 μm (and the capillary channel a total depth of about 130 μm) [17].

161 Next, the columns were modified with C₁₈ coating using ODS-DMA as described in detail
 162 previously [25]. Briefly, 10% ODS-DMA/toluene (v/v) was pumped through column at 60 °C for
 163 24h and washed with toluene, 50 % acetonitrile/toluene (v/v), and then acetonitrile. A typical SEM
 164 image of the NPAC is indicated in Fig .1. The properties of the NPAC are summarized in table 1.



165

166 **Fig .1.** SEM picture of pillars comprising the NPAC

167 **Table 1.** The NPAC properties.

Column length	Channel width	Pillar type	Pillar height	Pillar diameter	Inter pillar distance
20 cm	315 μm	Cylindrical	18 μm	5 μm	2.50 μm

168 **3.4. Measurements of the overloaded band profiles of naproxen and fenopfen on NPAC**

169 The standard stock solution of the chemicals was prepared in LC/MS grade methanol at a
 170 concentration of 1000 μg mL⁻¹. The solutions were stored at 4°C and heated to room temperature

171 before use. Sample containing naproxen and fenoprofen were prepared daily freshly via dilution
172 of stock solution with the used mobile phase (methanol/water) to get adequate concentration. The
173 overloading profiles of naproxen and fenoprofen were recorded at 230 and 215 nm, respectively.

174 **3.5. Determination of the adsorption isotherms by FA**

175 The appropriate chromatographic condition to obtain the adsorption isotherm was determined by
176 the shape of the recorded band profile. 30 % methanol/water (v/v) as the mobile phase at a flow-
177 rate of 1.0 μ l/min and the column temperature at 35 °C was used which lead to fronting and tailing
178 band shape for naproxen and fenoprofen, respectively.

179 Prior to the isotherm determinations, approximate values of the solubility of analytes were
180 determined. A concentration of 100 ppm was selected for naproxen and 200 ppm for fenoprofen
181 to avoid precipitation in the instrument. Two master solutions of each profen were prepared at 10
182 and 100% of the selected concentration. One pump of the HPLC instrument was used to deliver a
183 flow of the pure mobile phase (30 % methanol/water (v/v)) and two other pumps pumped a flow
184 of the 10% and 100% sample solutions into the NPAC. In case of fenoprofen, consecutive FA runs
185 were performed starting from the lowest to the highest concentrations. The opposite direction was
186 used in case of naproxen, i.e., the FA procedure started from the highest concentration and
187 continued to the lowest concentration. The breakthrough curves were recorded with a sufficiently
188 long time between each step (20 and 15 min for fenoprofen and naproxen, respectively) to allow
189 for the complete re-equilibration of the column. The detector was set at 230 nm for naproxen and
190 215 nm for fenoprofen.

191 **4. Results and discussion**

192 **4.1. Overloaded band (elution) profiles**

193 The elution profile of overloaded analytes contains information about the stationary phase and the
194 mobile phase.

195 Two set of samples containing different concentration of naproxen and fenoprofen were introduced
196 into the NPAC and elution profiles were recorded. Different compositions of methanol/water (35-

197 15% methanol/water (v/v) were tested as the mobile phase). The temperature of the column was
198 also varied (15-35 °C). Application of acetonitrile/water compositions resulted similar results.

199 A set of elution profiles was generated with different concentration of each analyte using 30 %
200 methanol/water (v/v) as the mobile phase at the column temperature of 35 °C. Typical results are
201 given in Fig.2.

202 As is common for overloading conditions [26, 27], we observed that the analytes band shapes were
203 dependent on the chromatographic conditions.

204 While naproxen exhibits a fronting band shape in most cases studied in the present paper (35%
205 methanol/water (v/v) at 15-35 °C ($A_s = -0.80 - (-1.1)$), 30 % methanol/water (v/v) at 15-35 °C
206 ($A_s = -0.11 - (-0.89)$) and 25 % methanol/water (v/v) at 25-35 °C ($A_s = -0.26 - (-0.29)$), the
207 fenoprofen peak is eluted with tailing in all studied conditions. The fronting peak of naproxen (see
208 Fig. 2) is assumed to emerge from an interaction between naproxen molecules (next to a weaker
209 interaction with the stationary phase) and the tailing peak of fenoprofen arises only from
210 interactions between the fenoprofen molecules and the stationary phase.

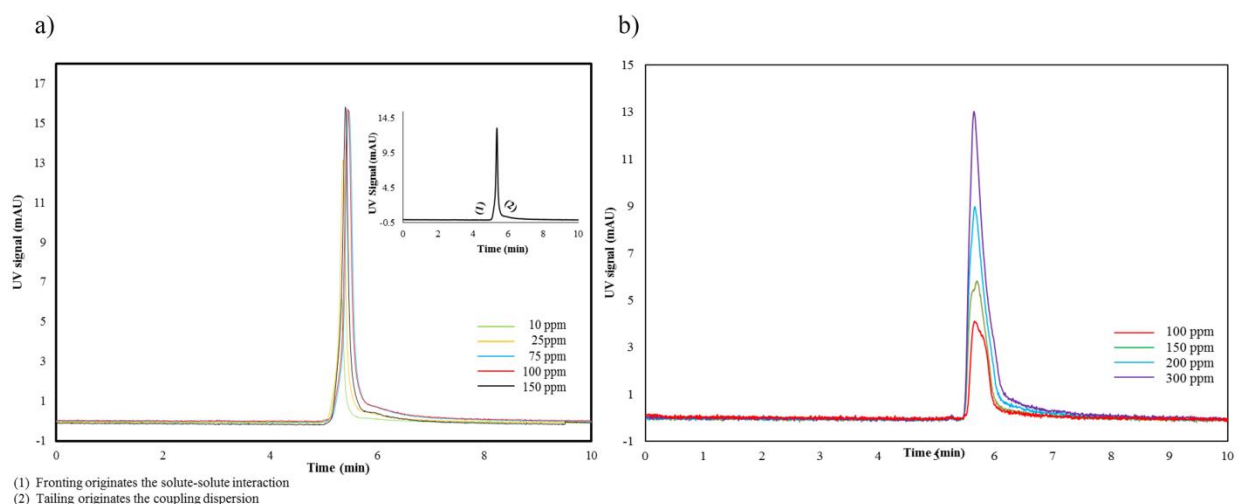
211 Using 15% methanol/water (v/v) as the mobile phase caused tailing peak for naproxen at 15-30 °C
212 ($A_s = 0.65-0.50$). This indicates that the interaction between naproxen molecules and the column
213 surface is stronger than the interaction between naproxen molecules when a mobile phase with
214 high water content is used. In fact, the higher water content in the mobile phase leads to a larger
215 number of high-energy sites on the stationary phase [28]. As a result, more interaction between
216 the analyte molecules and stationary phase surface is possible.

217 Naproxen is less retained than fenoprofen on the NPAC column. The elution order can be
218 understood by the degree of hydrophobicity. Naproxen with a lower octanol/water distribution
219 partition coefficient ($\log D = 2.99$) is eluted faster than fenoprofen ($\log D = 3.65$).

220 Figures 2a and 2b show that the band profiles of naproxen and fenoprofen are very different. NPAC
221 shows fronting peak when overloaded by naproxen at a concentration > 25 ppm ($A_s < 0$). Fig. 2a
222 depicts an upward concave isotherm and the increase of the amount injected does not change the
223 retention time significantly and leads to a few increase in the retention time of naproxen. This

224 observation can be explained by the anti-Langmuir adsorption behavior, where solute-solute
225 interactions cause increased retention as the sample load increases [29].

226 In contrast, for more hydrophobic drug (fenoprofen) in overloading conditions (concentration >
227 50 ppm) the tailing behavior ($A_s > 0$) was observed on NPAC. Fig. 2b corresponds to the concave
228 downward isotherm and the peak has the appearance of a triangle. The retention times move a bit
229 to shorter values with increasing sample size, as commonly observed [30-32]. Also, the extents of
230 the tailing increase with more sample load.



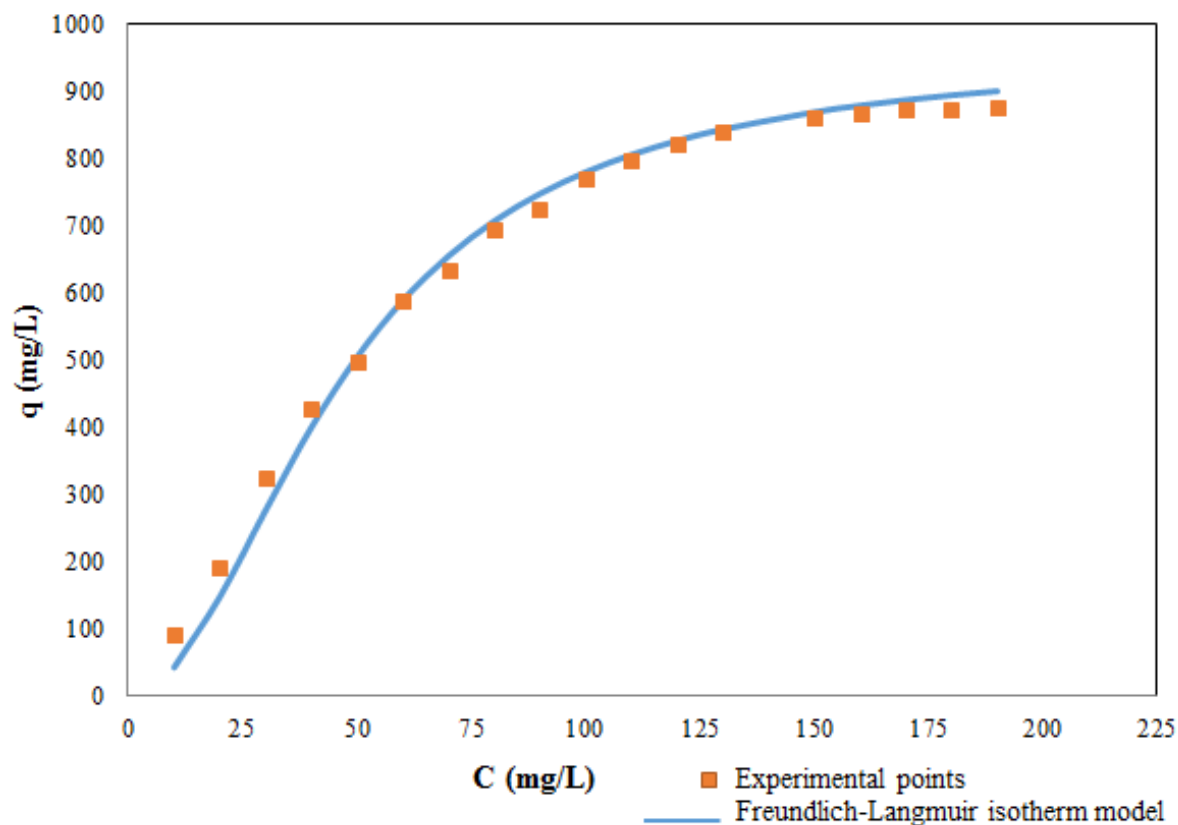
231
232 **Fig. 2.** Overloaded elution profiles of (a) naproxen at 230 nm and (b) fenoprofen at detected at 215 nm on the NPAC.
233 Other chromatographic conditions are: mobile phase: 30% methanol/water (v/v), column temperature: 35 °C, mobile
234 phase flow rate: 1.0 μ l/min.

235 4.2. The adsorption isotherm of fenoprofen: Langmuir-Freundlich isotherm model

236 The position and shape of overloaded band profiles recorded in LC depends directly on the
237 adsorption equilibrium isotherm of the compound between the stationary and the mobile phases.
238 Therefore, to understand the behavior of the selected pharmaceutical analytes on NPAC in
239 preparative RP-LC, adsorption isotherms of these analytes were measured. The obtained
240 breakthrough curves are indicated in Fig. 1S and Fig. 2S.

241 The adsorption isotherm models most frequently encountered in liquid chromatography are of
242 Langmuirian-type (Freundlich, Langmuir-Freundlich, Langmuir, Bi- Langmuir, Tri- Langmuir,
243 Toth, etc.) isotherm model. Fig. 3 shows the isotherm curve for the experimental adsorption of

244 fenoprofen on NPAC. The experimental adsorption data was best fitted by the Freundlich-
 245 Langmuir model. The obtained isotherm parameters are listed in table 2. At the low concentrations,
 246 the Langmuir-Freundlich model reduces to the classical Freundlich and in the case of a
 247 homogeneous surface (N=1), it reduces to the classical Langmuir model [33].



248

249 **Fig. 3.** The adsorption isotherm of fenoprofen on NPAC. Chromatography condition: mobile phase: 30%
 250 methanol/water (v/v), column temperature: 35 °C, mobile phase flow rate: 1.0 µl/min, detection: 215 nm.

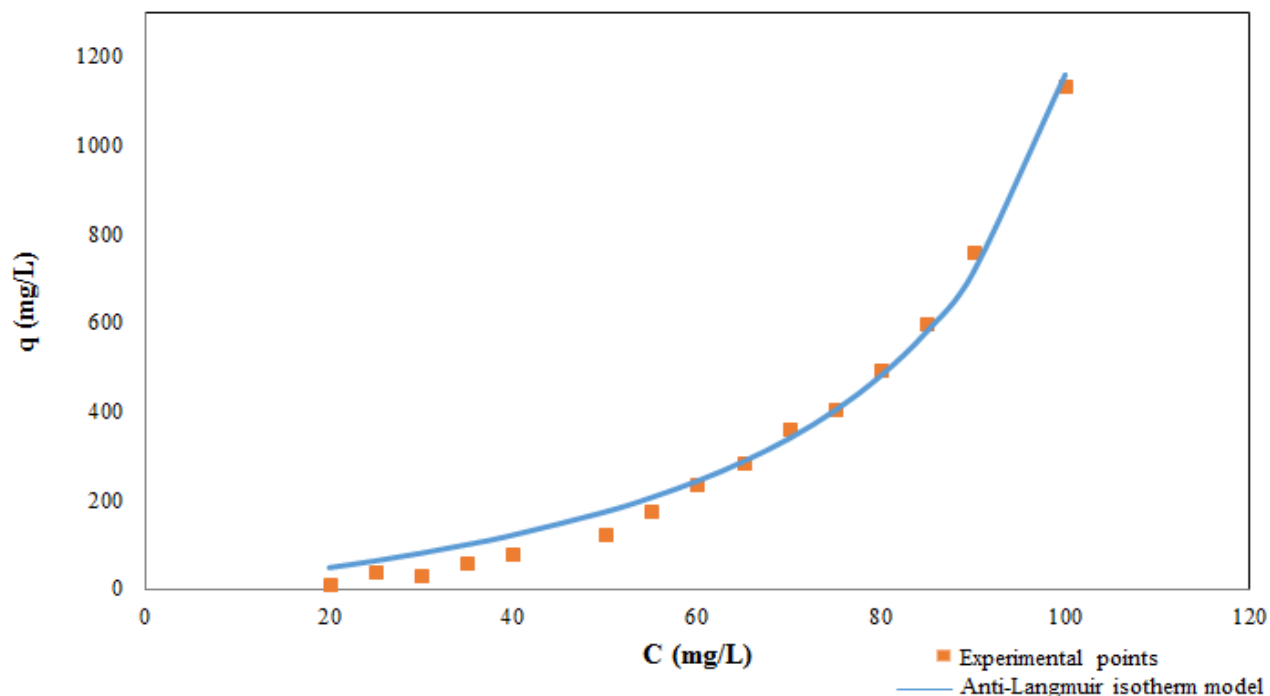
251 **Table 2.** The adsorption isotherm parameters obtained by fitting the experimental FA data of the fenoprofen on NPAC
 252 using Freundlich-Langmuir model.

Column saturation capacity (mg/L)	Affinity constant (L/mg)	Heterogeneity parameter	Regression Coefficient (R ²)
958.19	4.90*10 ⁻⁴	0.51	0.99

253

254 **4.3. The adsorption isotherm of naproxen: Anti-Langmuir isotherm model**

255 The fenopfen isotherm is concave downward for the entire investigated concentration range,
256 while the isotherm for naproxen is concave upward (Fig.4). The downward concave is mostly
257 observed in liquid–solid or liquid-liquid equilibrium, however, the upward concave isotherm is
258 less common in liquid chromatography [22].



259

260 **Fig.4.** The adsorption isotherm of naproxen on NPAC. Chromatography condition: mobile phase: 30%
261 methanol/water (v/v), column temperature: 35 °C, mobile phase flow rate: 1.0 µl/min, detection: 230 nm.

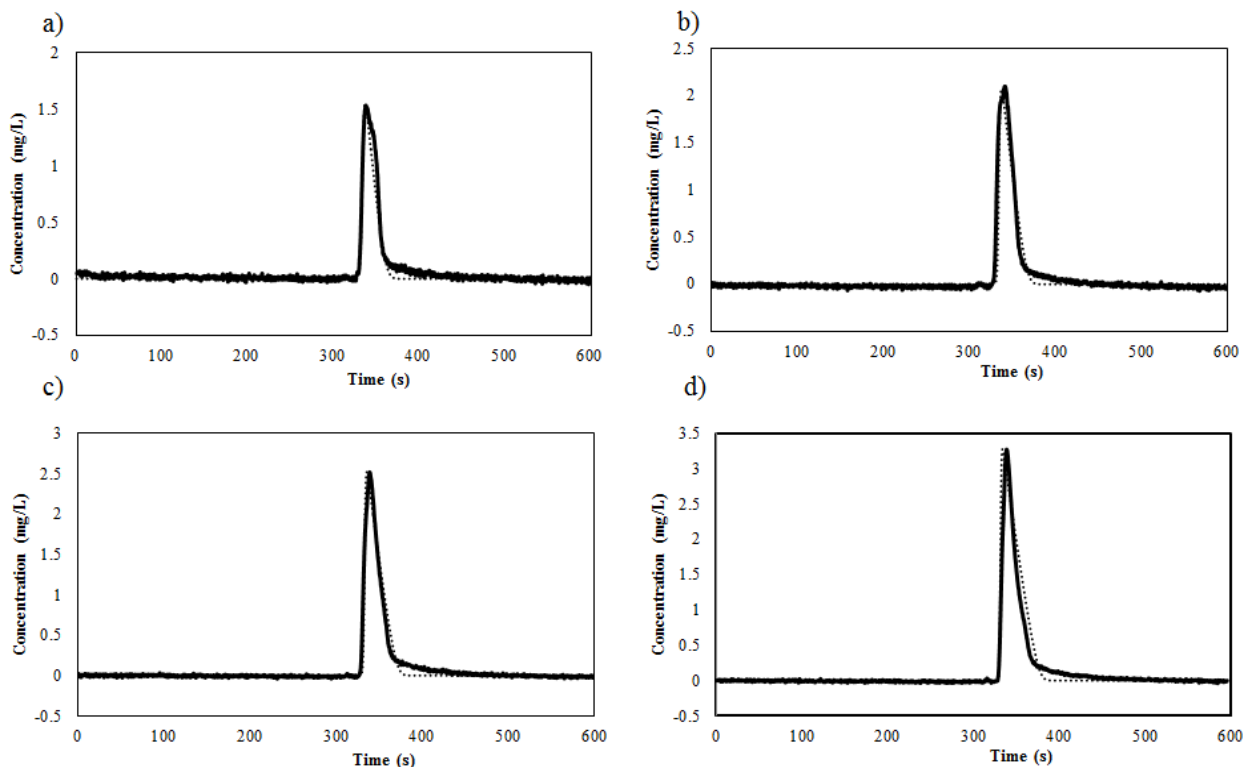
262 In the upward concave situation, the concentration in the stationary phase at equilibrium increases
263 faster than the concentration in the mobile phase. This means that a second molecule is more
264 strongly adsorbed than a first one (or more general: adding a molecule to n molecules) which
265 commonly indicates the existence of attractive interactions between the adsorbed molecules. Anti-
266 Langmuir adsorption model describes the upward concave isotherms and accounts for the
267 adsorption behavior due to solute–solute interactions [34]. The experimental data were fitted into
268 several models and the best result was obtained by anti-Langmuir isotherm model. The parameters
269 were obtained through nonlinear least-squares fitting ($R^2 = 0.99$, see table 3 for obtained
270 parameters).

271 **Table 3.** The adsorption isotherm parameters obtained by fitting the experimental FA data of the naproxen on NPAC
272 using anti-Langmuir model.

A	B	Regression Coefficient (R ²)
2.01	8.22*10 ⁻³	0.99

273 4.4. Validation of isotherm models

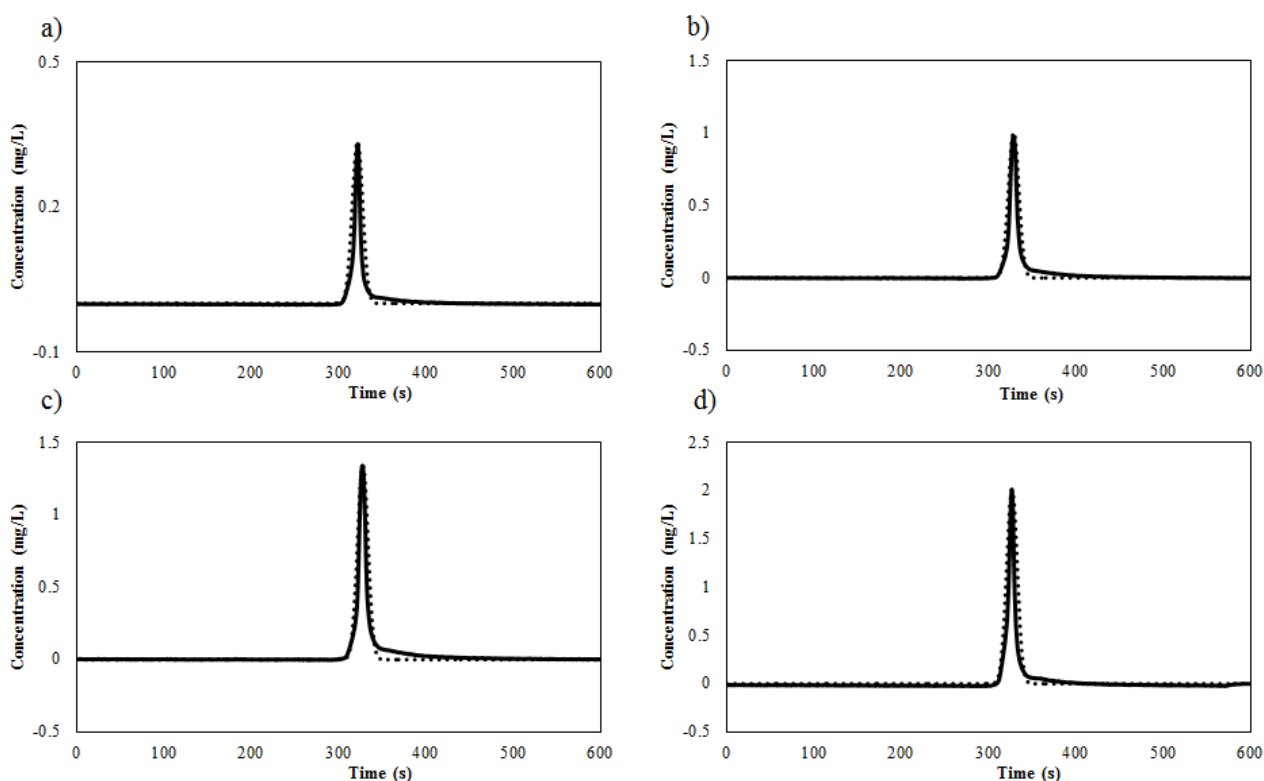
274 According to Fig. 3, the isotherm model that accounts best for the adsorption data of fenoprofen
275 on the NPAC is the Langmuir-Freundlich model. With the obtained parameters, it is also possible
276 to predict the peak shape at a given concentration and mobile phase velocity. The experimentally
277 obtained and predicted curves are depicted in Fig. 5 (dashed lines). The calculated profiles were
278 derived using the equilibrium-dispersive model (see section 2.2). As can be noticed, the curves are
279 in qualitative agreement. This result confirms that the selected model is adequate. There is some
280 minor deviation near the baseline, which can most likely be predominantly attributed to coupling
281 dispersion between the PAC outlet and the detection capillary [17].



282

283 **Fig. 5.** Experimental (solid lines) and calculated band profiles (dotted lines) of fenoprofen on NPAC. a) 100 mg/L b)
284 150 mg/L c) 200 mg/L d) 300 mg/L. Experimental conditions are the same as in Fig. 3. The best isotherm
285 parameters are listed in table 2.

286 The validity of the selected isotherm model in case of naproxen was also checked by comparing
287 calculated and experimental band profiles (Fig. 6). As can be seen, the naproxen band profile on
288 NPAC is well predicted by the anti-Langmuir model in the whole concentration range. The
289 observed minor deviation at the peak rear can again most probably be attributed to coupling
290 dispersion.



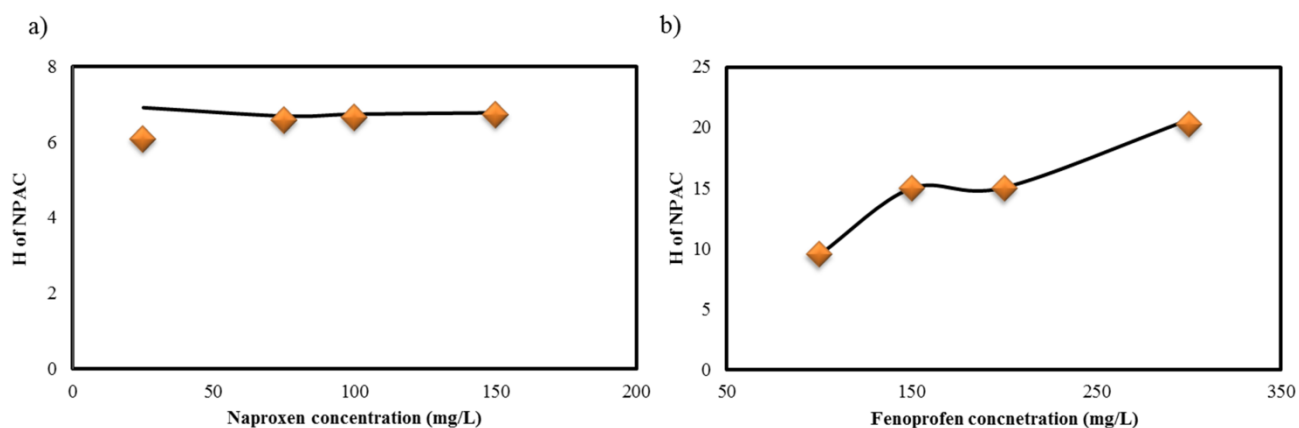
291
292 **Fig. 6.** Experimental (solid lines) and calculated band profiles (dotted lines) of naproxen on NPAC a) 25 mg/L b) 75
293 mg/L c) 100 mg/L d) 150 mg/L. Experimental conditions are the same as in Fig. 4. The best isotherm parameters are
294 listed in table 3.

295 4.5. The column efficiency in overloaded condition

296 For a linear isotherm the plate number is independent of the sample concentration. The elution
297 bands studied here are operated in nonlinear condition at overloading conditions, with the peak

298 width determined by the isotherm curvature [35]. As expected, the column efficiency decreases
299 with increasing concentration. The obtained result for naproxen has been showed in Fig. 7a,
300 showing a modest sensitivity to concentration. A much might higher sensitivity was observed for
301 fenoprofen (Fig.7b).

302 Using predictable band shapes, one can also assess the separation performance for given
303 conditions. To this end, the plate heights of the calculated peaks calculated, and subsequently
304 compared to the experimentally obtained values. As is shown in Fig.7, an excellent agreement can
305 be observed in the whole concentration range of both analytes, except 25 ppm concentration, which
306 indicates the selected isotherm models can describe the NPAC behavior well.



307

308 **Fig. 7.** Plate height as a function of analyte concentration calculated using experimentally obtained (points) and
309 calculated values (solid lines) using the method of moments for a) naproxen b) fenoprofen. Experimental conditions
310 are the same as in Fig.2.

311 5. Concluding remarks

312 In liquid chromatography, the adsorption isotherms offer a picture of the process occurring inside
313 the column. These are key importance at a preparative and production scale, therefore, in this study
314 the parameters of the adsorption equilibrium isotherms on NPAC using naproxen and fenoprofen
315 as two model compounds were determined. The adsorption mechanism of naproxen is well
316 described by the anti-Langmuir isotherm model. The adsorption of fenoprofen exhibited a
317 Langmuirian behavior. Injection of naproxen to the NPAC on the overloaded condition led to a
318 fronting peak, however, injection of high concentration of fenoprofen created a tailing peak. The

319 band shape and isotherm model is determined based on the analytes and the stationary phase as
320 well as mobile phase. In the selected mobile phase, naproxen showed that solute–solute interaction
321 more than solute-stationary phase interaction. As a result, naproxen eluted with a fronting peak
322 and its behavior on NPAC is in line with the anti-Langmuir isotherm model. On the contrary,
323 fenoprofen showed a higher tendency to interact with NPAC surface, resulting in Langmuirian
324 behavior and a tailing peak. The band profiles and plate heights can be well predicted for
325 overloading conditions. The excellent agreement between experimental and predicted results for
326 both analytes indicates that the selected isotherm models are well suitable.

327 **Acknowledgments**

328 The authors gratefully acknowledge support from Vrije Universiteit Brussel and Shahid Beheshti
329 University.

330 **Conflicts of interest**

331 Wim De Malsche is (co-)founder and shareholder of PharmaFluidics, a company that
332 commercializes pillar array columns.

References

- [1] X. Ye, D. Cao, F. Song, G. Fan, F. Wu, Preparative separation of nine flavonoids from *Pericarpium Citri Reticulatae* by preparative-HPLC and HSCCC, *Sep. Sci. Technol.* 51 (2016) 807-815.
- [2] S. Schmitz, D.L. Schönfeld, B. Freitag, C. Götzberger-Schad, M. Fischer, L. Linden, Keeping pace with the increasing demand for high quality drug candidates in pharmaceutical research: Development of a new two-step preparative tandem high performance chromatographic system for the purification of antibodies, *J. Chromatogr. B* 1104 (2019) 18-28.
- [3] M. Lal, R. Bhushan, Analytical and semi-preparative enantioresolution of (RS)-ketorolac from pharmaceutical formulation and in human plasma by HPLC, *Biomed. Chromatogr.* 30 (2016) 1526-1534.
- [4] A.E. Ribeiro, N.S. Graça, L.S. Pais, A.E. Rodrigues, Preparative separation of ketoprofen enantiomers: Choice of mobile phase composition and measurement of competitive adsorption isotherms, *Sep. Purif. Technol.* 61 (2008) 375-383.
- [5] M. Enmark, J. Bagge, J. Samuelsson, L. Thunberg, E. Örnskov, H. Leek, F. Limé, T. Fornstedt, Analytical and preparative separation of phosphorothioated oligonucleotides: columns and ion-pair reagents, *Anal. Bioanal. Chem.* 412 (2020) 299-309.
- [6] X. Meng, Y. Li, C. Lu, M. Zhao, M. Li, S. Wang, C. Zhao, B. Lin, L. Shang, Z. Chu, Purification and antioxidant capacity analysis of anthocyanin glucoside cinnamic ester isomers from *Solanum nigrum* fruits, *J. Sep. Sci.* 43 (2020) 2311-2320.
- [7] J. Samuelsson, F.F. Eiriksson, D. Åsberg, M. Thorsteinsdóttir, T. Fornstedt, Determining gradient conditions for peptide purification in RPLC with machine-learning-based retention time predictions, *J. Chromatogr. A* 1598 (2019) 92-100.
- [8] D. Åsberg, A.L. Weinmann, T. Leek, R.J. Lewis, M. Klarqvist, M. Leško, K. Kaczmarek, J. Samuelsson, T. Fornstedt, The importance of ion-pairing in peptide purification by reversed-phase liquid chromatography, *J. Chromatogr. A* 1496 (2017) 80-91.

- [9] H. Li, X. Jiang, W. Xu, Y. Chen, W. Yu, J. Xu, Numerical determination of non-Langmuirian adsorption isotherms of ibuprofen enantiomers on Chiralcel OD column using ultraviolet–circular dichroism dual detector, *J. Chromatogr. A* 1435 (2016) 92-99.
- [10] F. Gritti, G. Guiochon, Hydrophilic interaction chromatography: A promising alternative to reversed-phase liquid chromatography systems for the purification of small protonated bases, *J. Sep. Sci.* 38 (2015) 1633-1641.
- [11] A. Seebach, A. Seidel-Morgenstern, Enantioseparation on molecularly imprinted monoliths—Preparation and adsorption isotherms, *Anal. Chim. Acta* 591 (2007) 57-62.
- [12] E. Naghdi, A.R. Fakhari, M. Baca, W. De Malsche, Simultaneous enantioseparation of nonsteroidal anti-inflammatory drugs by a one-dimensional liquid chromatography technique using a dynamically coated chiral porous silicon pillar array column, *J. Chromatogr. A* 1615 (2020) 460752.
- [13] G. Nys, G. Cobraiville, M. Fillet, Multidimensional performance assessment of micro pillar array column chromatography combined to ion mobility-mass spectrometry for proteome research, *Anal. Chim. Acta* 1086 (2019) 1-13.
- [14] J.O. De Beeck, J. Pauwels, A. Staes, N. Van Landuyt, D. Van Haver, W. De Malsche, G. Desmet, A. Argentini, L. Martens, P. Jacobs, Digging deeper into the human proteome: A novel nanoflow LCMS setup using micro pillar array columns (μ PACTM), *bioRxiv* (2018) 472134.
- [15] W.D. Malsche, H. Gardeniers, G. Desmet, Experimental study of porous silicon shell pillars under retentive conditions, *Anal. Chem.* 80 (2008) 5391-5400.
- [16] L. Zhang, B. Majeed, L. Lagae, P. Peumans, C. Van Hoof, W. De Malsche, Ion-pair reversed-phase chromatography of short double-stranded deoxyribonucleic acid in silicon micro-pillar array columns: Retention model and applications, *J. Chromatogr. A* 1294 (2013) 1-9.
- [17] W. De Malsche, S. De Bruyne, J.O. De Beek, P. Sandra, H. Gardeniers, G. Desmet, F. Lynen, Capillary liquid chromatography separations using non-porous pillar array columns, *J. Chromatogr. A* 1230 (2012) 41-47.

- [18] Y. Song, K. Takatsuki, T. Sekiguchi, T. Funatsu, S. Shoji, M. Tsunoda, Rapid quantitative method for the detection of phenylalanine and tyrosine in human plasma using pillar array columns and gradient elution, *Amino Acids* 48 (2016) 1731-1735.
- [19] G. Guiochon, Preparative liquid chromatography, *J. Chromatogr. A* 965 (2002) 129-161.
- [20] G. Zhong, P. Sajonz, G. Guiochon, Shock layer theory and concentration dependence of the axial dispersion and the mass-transfer rate coefficients, *Ind.Eng. Chem. Res.* 36 (1997) 506-509.
- [21] D.M. Ruthven, Principles of adsorption and adsorption processes, John Wiley & Sons 1984.
- [22] A. Cavazzini, G. Bardin, K. Kaczmarski, P. Szabelski, M. Al-Bokari, G. Guiochon, Adsorption equilibria of butyl- and amylbenzene on monolithic silica-based columns, *J. Chromatogr. A* 957 (2002) 111-126.
- [23] F. Gritti, G. Guiochon, Effect of the ionic strength of salts on retention and overloading behavior of ionizable compounds in reversed-phase liquid chromatography: I. XTerra-C18, *J. Chromatogr. A* 1033 (2004) 43-55.
- [24] M. Czok, G. Guiochon, The physical sense of simulation models of liquid chromatography: propagation through a grid or solution of the mass balance equation, *Anal. Chem.* 62 (1990) 189-200.
- [25] S. Futagami, T. Hara, H. Ottevaere, H. Terry, G.V. Baron, G. Desmet, W. De Malsche, Chromatographic study of the structural properties of mesoporous silica layers deposited on radially elongated pillars, *J. Chromatogr. A* 1595 (2019) 58-65.
- [26] W. Lao, J. Gan, Characterization of warfarin unusual peak profiles on oligoproline chiral high performance liquid chromatography columns, *J. Chromatogr. A* 1217 (2010) 6545-6554.
- [27] M.F. Wahab, J.K. Anderson, M. Abdelrady, C.A. Lucy, Peak distortion effects in analytical ion chromatography, *Anal. Chem.* 86 (2014) 559-566.

- [28] F. Gritti, G. Guiochon, Effect of the mobile phase composition on the isotherm parameters and the high concentration band profiles in reversed-phase liquid chromatography, *J. Chromatogr. A* 995 (2003) 37-54.
- [29] I. Baškurova, V. Olšauskaitė, A. Padarauskas, Overloading study of ionized compounds in hydrophilic interaction chromatography, *Chemija*, 29 (2018).
- [30] N.H. Davies, M.R. Euerby, D.V. McCalley, A study of retention and overloading of basic compounds with mixed-mode reversed-phase/cation-exchange columns in high performance liquid chromatography, *J. Chromatogr. A* 1138 (2007) 65-72.
- [31] S.M. Buckenmaier, D.V. McCalley, M.R. Euerby, Overloading study of bases using polymeric RP-HPLC columns as an aid to rationalization of overloading on silica-ODS phases, *Anal. Chem.* 74 (2002) 4672-4681.
- [32] L. Wang, R.K. Marcus, Overload Effects in Reversed Phase Protein Separations using Capillary-Channeled Polymer Fiber Columns, *Biotechnol. Prog.* 34 (2018) 1221-1233.
- [33] G. Guiochon, S. Golshan-Shirazi, A.M. Katti, Fundamentals of preparative and nonlinear chromatography, Academic Press, New York, 1994.
- [34] F. Gritti, G. Guiochon, Overloaded elution band profiles of ionizable compounds in reversed-phase liquid chromatography: Influence of the competition between the neutral and the ionic species, *J. Sep. Sci.* 31 (2008) 3657-3682.
- [35] G. Guiochon, S. Golshan-Shirazi, A. Jaulmes, Computer simulation of the propagation of a large-concentration band in liquid chromatography, *Anal. Chem.* 60 (1988) 1856-1866.

